

# A mathematical model for contaminant adsorption in packed columns using nonlinear mass transfer

F. Font<sup>1</sup>, A. Estop<sup>2</sup>, M. Calvo-Schwarzwalder<sup>3</sup>, A. Valverde<sup>4</sup>, T.G. Myers<sup>5</sup>

<sup>1</sup> Department of Fluid Mechanics, Universitat Politècnica de Catalunya,  
08019 Barcelona, Spain

`francesc.font@upc.edu`

<sup>2</sup> Universitat Autònoma de Barcelona, Campus de Bellaterra, Edifici C,  
08193 Bellaterra, Barcelona, Spain.

`albert.estop@autonoma.cat`

<sup>3</sup> College of Interdisciplinary Studies, Zayed University,  
P.O. Box 144534 Abu Dhabi, United Arab Emirates

`marc.schwarzwalder@zu.ac.ae`

<sup>4</sup> Department of Chemical Engineering, Universitat Politècnica de Catalunya,  
08028 Barcelona, Spain

`abel.valverde@upc.edu`

<sup>5</sup> Centre de Recerca Matemàtica, Campus de Bellaterra, Edifici C,  
08193 Bellaterra, Barcelona, Spain.

`tmyers@crm.cat`

**Abstract.** We propose a mathematical model for describing column adsorption processes where large amounts of contaminant are removed from a carrier gas. The large mass loss causes velocity and pressure to be variables which must then be determined along with the contaminant and gas concentrations and adsorbed quantity. The adsorption rate is described using a Langmuir sink, which is physically more sensible than the linear sink used in a previous study. The proposed model is solved numerically and using a traveling wave approach. The analytical solutions are consistent with previous models with fixed gas velocity and provide excellent agreement when validated against experimental data.

**Keywords:** Contaminant removal, Pollutant removal, Adsorption, Fluid dynamics, Langmuir equation

## 1 Introduction

Column sorption is a process where a fluid, typically formed by a contaminant and a carrier fluid, is forced to flow through a column that is packed with a porous adsorbent material. The contaminant then attaches to the adsorbent until an equilibrium state is reached, where the concentration of contaminant measured at the outlet is equal to that of the inlet. When trace amounts are removed, such that the pressure and velocity of the carrier are not affected the

process is relatively well understood [1,2,3,4]. When a significant quantity of the mixture is removed these previous models no longer hold. Myers and Font [5] proposed an extension that accounts for larger amounts of contaminant, where the fluid velocity  $u$  and pressure  $p$  are unknown quantities to be determined along with the contaminant and carrier gas concentration profiles, respectively  $c_1$  and  $c_2$ , and adsorbed amount per unit mass of adsorbent  $q$ . In [5] a standard linear kinetic model was employed to describe the mass removal however this neglects desorption and does not explicitly account for the presence of contaminant with the result that, theoretically, adsorption may occur without any contaminant to be adsorbed. The Langmuir model [6] does not have these limitations, which is why we propose extending the model of [5] using this kinetic model.

## 2 Mathematical formulation

We consider a column of length  $L$  that is packed with a porous material. A gas mixture with fixed contaminant and carrier gas volume fractions  $\phi_1$  and  $\phi_2$  is introduced at the inlet at a constant velocity  $u_{in}$  and is adsorbed by the adsorbent as it flows towards the outlet, where the concentration of contaminant is measured. We assume that the pressure at the inlet is higher than the pressure at the outlet,  $p_{in} = p_a + \Delta p$  and  $p_{out} = p_a$ , where  $p_a$  is the ambient pressure. To maintain a constant mass flux, the pressure drop must be a function of time, we write  $\Delta p = P(t)$ . Using the ideal gas law, for a given volume fraction  $\phi_i$ , the concentration,  $c$ , of species  $i$  just outside the inlet is

$$\begin{aligned} c_i(0^-, t) &= \frac{\phi_i p_{in}(t)}{R_g T} = \frac{\phi_i}{R_g T} (p_a + P(t)) \\ &= \frac{\phi_i p_a}{R_g T} \left( 1 + \frac{P(t)}{p_a} \right) = c_{i0} \left( 1 + \frac{P(t)}{p_a} \right), \end{aligned} \quad (1)$$

where  $T$  the temperature and  $R_g$  is the universal gas constant. If the pressure drop is small ( $P \ll p_a$ ) then the inlet concentrations can be considered approximately constant.

Following the model proposed by Myers and Font [5], we consider all the quantities averaged over the column cross-section and therefore consider only one spatial variable  $x$ , representing the distance from the column inlet. Assuming that we are in a Darcy flow regime (this is shown in [5]), the dimensional model consists of the following set of equations:

$$\frac{\partial c_1}{\partial t} + \frac{\partial}{\partial x}(uc_1) = D \frac{\partial^2 c_1}{\partial x^2} - \rho_q \frac{\partial q}{\partial t}, \quad (2a)$$

$$\frac{\partial c_2}{\partial t} + \frac{\partial}{\partial x}(uc_2) = D \frac{\partial^2 c_2}{\partial x^2}, \quad (2b)$$

$$p = R_g T(c_1 + c_2), \quad -\frac{\partial p}{\partial x} = \frac{\mu}{\kappa} u, \quad \frac{\partial q}{\partial t} = \dot{Q}, \quad (2c)$$

where  $D$  is the mass diffusivity,  $\rho_q$  is an effective density related to the porosity and density of the adsorbent,  $\mu$  is the dynamic viscosity, and  $\kappa$  is the permeability. The expression of  $\dot{Q}$  depends on the underlying mass transfer model. The Langmuir model is

$$\dot{Q}(q, c_1) = k_{ad}c_1(q_m - q) - k_{de}q, \quad (3)$$

where  $k_{ad}$  and  $k_{de}$  are the adsorption and desorption rates and  $q_m$  represents the maximum amount that may be adsorbed. Equilibrium is reached when both processes balance and thus contaminant concentration does not change with respect to its inlet value. Solving  $\dot{Q} = 0$  to find the equilibrium amount  $q_e$  yields the Langmuir isotherm

$$q_e = \frac{q_m K_L c_{10}}{K_L c_{10} + 1}, \quad (4)$$

where  $K_L = k_{ad}/k_{de}$  is referred to as the Langmuir equilibrium constant.

The boundary conditions for the concentrations are

$$u_{in}c_i(0^-, t) = \left(uc_i - D\frac{\partial c_i}{\partial x}\right)\Big|_{x=0^+}, \quad \frac{\partial c_i}{\partial x}\Big|_{x=L} = 0 \quad (i = 1, 2). \quad (5)$$

Additionally, for the pressure we have

$$p(0, t) = p_{in}(t) \quad p(L, t) = p_a. \quad (6)$$

Finally, the initial conditions are

$$c_1(x, 0) = q(x, 0) = 0, \quad p(x, 0) = p_0(x), \quad c_2(x, 0) = \frac{p_0(x)}{R_g T}, \quad (7)$$

where  $p_0(x) = p_a + (1 - x/L)P(0)$ . Following Myers and Font [5], we scale the variables with the following:

$$c_i \sim c_{i0}, \quad q \sim q_m, \quad u \sim u_{in}, \quad p - p_a \sim \mathcal{P}, \quad x \sim \mathcal{L}, \quad t \sim \tau, \quad (8)$$

where

$$\mathcal{P} = \frac{\mu \mathcal{L} u_{in}}{\kappa}, \quad \mathcal{L} = \frac{u_{in} \tau c_{10}}{\rho_q q_m}, \quad \tau = \frac{1}{c_{10} k_{ad}}. \quad (9)$$

Upon indicating the scaled quantities with a hat notation and following the nomenclature of [5], the non-dimensional formulation of the problem reads

$$\delta_1 \frac{\partial \hat{c}_1}{\partial \hat{t}} + \frac{\partial}{\partial \hat{x}}(\hat{u} \hat{c}_1) = \delta_2 \frac{\partial^2 \hat{c}_1}{\partial \hat{x}^2} - \frac{\partial \hat{q}}{\partial \hat{t}}, \quad \delta_1 \frac{\partial \hat{c}_2}{\partial \hat{t}} + \frac{\partial}{\partial \hat{x}}(\hat{u} \hat{c}_2) = \delta_2 \frac{\partial^2 \hat{c}_2}{\partial \hat{x}^2}, \quad (10a)$$

$$1 + \delta_3 \hat{p} = \delta_{45} \hat{c}_1 + \delta_4 \hat{c}_2, \quad -\frac{\partial \hat{p}}{\partial \hat{x}} = \hat{u}, \quad \frac{\partial \hat{q}}{\partial \hat{t}} = \hat{c}_1(1 - \hat{q}) - \delta_6 \hat{q}, \quad (10b)$$

where

$$\delta_1 = \frac{\mathcal{L}}{\mathcal{U} \tau}, \quad \delta_2 = \frac{D}{\mathcal{U} \mathcal{L}}, \quad \delta_3 = \frac{\mathcal{P}}{p_a}, \quad (11)$$

$$\delta_4 = \phi_2, \quad \delta_5 = \frac{\phi_1}{\phi_2}, \quad \delta_{45} = \delta_4 \delta_5 = \phi_1, \quad \delta_6 = \frac{1}{K_L c_{10}}.$$

The non-dimensional boundary conditions are

$$1 + \delta_3 \hat{P}(\hat{t}) = \left( \hat{u} \hat{c}_j - \delta_2 \frac{\partial \hat{c}_j}{\partial \hat{x}} \right) \Big|_{\hat{x}=0}, \quad \frac{\partial \hat{c}_j}{\partial \hat{x}} \Big|_{\hat{x}=\hat{L}} = 0 \quad (j = 1, 2), \quad (12a)$$

$$\hat{p}(0, \hat{t}) = \hat{P}(\hat{t}), \quad \hat{p}(\hat{L}, \hat{t}) = 0, \quad \hat{p}(\hat{x}, 0) = (\hat{L} - \hat{x}) \hat{P}(0), \quad (12b)$$

$$\hat{c}_1(\hat{x}, 0) = \hat{q}(\hat{x}, 0) = 0, \quad \delta_4 \hat{c}_2(\hat{x}, 0) = 1 + \delta_3 \hat{p}(\hat{x}, 0), \quad (12c)$$

with  $\hat{L} = L/\mathcal{L}$  and  $\hat{P} = P/\mathcal{P}$ .

The parameters  $\delta_1$  and  $\delta_2$  are the Damköhler and inverse Péclet numbers,  $\delta_3$  is the relative pressure,  $\delta_4$ , is the volume fraction of carrier gas in the mixture before entering the column,  $\delta_5$  is the ratio of the volume fractions, and  $\delta_6$  relates adsorption and desorption. Following the discussion of [5], we assume  $\delta_1, \delta_2, \delta_3 \ll 1$  so that the corresponding terms are negligible to leading order.

To retrieve the fixed velocity model provided in [2], we will have to take the limits  $\phi_1 = \delta_{45} \rightarrow 0$  and  $\phi_2 = \delta_4 \rightarrow 1$ .

### 3 Solution Methods

#### 3.1 Traveling wave solution

These kinds of models may typically be solved using a traveling wave approach [1,2,3,4,5]. Upon neglecting terms of order  $\delta_1, \delta_2, \delta_3$ , and writing  $\delta_4$  and  $\delta_5$  in terms of the contaminant void fraction  $\phi_1$ , the problem reduces to

$$\frac{\partial}{\partial \hat{x}}(\hat{u} \hat{c}_1) = -\frac{\partial \hat{q}}{\partial \hat{t}}, \quad \frac{\partial}{\partial \hat{x}}(\hat{u} \hat{c}_2) = 0, \quad (13a)$$

$$1 = \phi_1 \hat{c}_1 + (1 - \phi_1) \hat{c}_2, \quad -\frac{\partial \hat{p}}{\partial \hat{x}} = \hat{u}, \quad \frac{\partial \hat{q}}{\partial \hat{t}} = \hat{c}_1(1 - \hat{q}) - \delta_6 \hat{q}. \quad (13b)$$

From the reduced equations we find

$$\hat{c}_2 = \frac{1 - \phi_1 \hat{c}_1}{1 - \phi_1}, \quad \hat{u} = \frac{1 - \phi_1}{1 - \phi_1 \hat{c}_1}, \quad (14)$$

where the first comes from rearranging Eq. (13b.i) and the second from integrating Eq. (13a.ii) and applying the boundary conditions at  $\hat{x} = 0$ . The problem then reduces to solving

$$\frac{\partial}{\partial \hat{x}} \left( \frac{(1 - \phi_1) \hat{c}_1}{1 - \phi_1 \hat{c}_1} \right) = -\frac{\partial \hat{q}}{\partial \hat{t}}, \quad \frac{\partial \hat{q}}{\partial \hat{t}} = \hat{c}_1(1 - \hat{q}) - \delta_6 \hat{q}. \quad (15)$$

Now we introduce the traveling wave coordinate  $\eta = \hat{x} - \hat{L} - \hat{v}(\hat{t} - \hat{t}_{1/2})$ , where  $\hat{v}$  is constant and  $\hat{t}_{1/2}$  is the (dimensionless) time when the outlet concentration is half of the inlet value,  $c_1 = c_{10}/2$ . Upon defining  $(1 - \phi_1) \hat{c}_1 / (1 - \phi_1 \hat{c}_1) = F(\eta)$  and  $\hat{q} = G(\eta)$  and denoting derivatives with respect to  $\eta$  with primes, the problem becomes

$$F' = \hat{v} G', \quad -\hat{v} G' = \frac{F(1 - G)}{1 - \phi_1(1 - F)} - \delta_6 G, \quad (16)$$

where we impose  $F \rightarrow 1$ , (i.e.  $\hat{c}_1 \rightarrow 1$ )  $G \rightarrow 1/(1 + \delta_6) = G_e$  as  $\eta \rightarrow -\infty$  (equilibrium far behind the wavefront) and  $F, G \rightarrow 0$  as  $\eta \rightarrow \infty$  (no free or adsorbed contaminant far ahead of the wavefront). Note,  $\hat{c}_1 = 1/2$  at  $\eta = 0$  yields the additional condition  $F(0) = (1 - \phi_1)/(2 - \phi_1) = F_{1/2}$ . Using these conditions, we can solve the problem and find

$$G = \frac{F}{\hat{v}}, \quad \hat{v} = \frac{1}{G_e} = 1 + \delta_6, \quad (17)$$

and  $F$  is given implicitly by the equation

$$-\frac{\eta}{1 + \delta_6} = \frac{1 - \phi_1}{1 + \phi_1 \delta_6} \ln \left| \frac{F}{F_{1/2}} \right| - \frac{1}{1 + \phi_1 \delta_6} \ln \left| \frac{1 - F}{1 - F_{1/2}} \right|. \quad (18)$$

In terms of  $\hat{c}_1$  this yields

$$-\frac{\eta}{1 + \delta_6} = \frac{1}{1 + \phi_1 \delta_6} \ln \left| \frac{\hat{c}_1}{1 - \hat{c}_1} \right| - \frac{\phi_1}{1 + \phi_1 \delta_6} \ln \left| \frac{(2 - \phi_1)\hat{c}_1}{1 - \phi_1 \hat{c}_1} \right|. \quad (19)$$

This method determines  $\hat{c}_1$ ,  $\hat{c}_2$ ,  $\hat{q}$ , and  $\hat{u}$ . Their profiles are shown in Fig. 1 and later discussed in section §3.3. The form in which Eq. (19) is presented allows the fixed velocity model to be easily retrieved by taking the limit  $\phi_1 \rightarrow 0$ . This limit is also discussed in §3.3

At this point, the pressure is the only quantity that has not been determined. We find it by integrating Eq. (13b.ii) and applying  $\hat{p} = 0$  at  $\hat{x} = \hat{L}$ . The pressure drop  $\hat{P}$  may then be found by applying the boundary condition at the inlet. We find

$$\hat{p} = \int_{\hat{x}}^{\hat{L}} \frac{1 - \phi_1}{1 - \phi_1 \hat{c}_1(\xi, \hat{t})} d\xi, \quad \hat{P}(\hat{t}) = \int_0^{\hat{L}} \frac{1 - \phi_1}{1 - \phi_1 \hat{c}_1(\xi, \hat{t})} d\xi. \quad (20)$$

Upon substituting  $\eta(\hat{L}, t) = \hat{v}(\hat{t} - \hat{t}_{1/2})$ , we find the implicit breakthrough model

$$\hat{t} = \hat{t}_{1/2} + f\left(\hat{c}_1(\hat{L}, \hat{t})\right) \Rightarrow t = t_{1/2} + \frac{1}{k_{ad}c_{10}} f\left(\frac{c_1(L, t)}{c_{10}}\right), \quad (21)$$

where  $f(\cdot)$  is defined as the right-hand side of Eq. (19).

### 3.2 Numerical solution

We expect  $\delta_3 = \mathcal{O}(10^{-2})$ , hence setting  $\delta_3 = 0$  suggests errors of the order of 1%. Upon doing this, the model unknowns reduce to  $\hat{c}_1$ ,  $\hat{q}$  and  $\hat{u}$ , while  $\hat{c}_2$  and  $\hat{p}$  become passive variables that can be obtained once  $\hat{c}_1$ ,  $\hat{q}$  and  $\hat{u}$  are known. Then, we can easily adapt the numerical method developed in [5], which is based on solving for  $\hat{c}_1$ ,  $\hat{q}$  and  $\hat{u}$  using second-order central finite differences in space and explicit Euler in time, while  $\hat{c}_2$  and  $\hat{p}$  are constructed *a posteriori*. Note that this approach retains the terms with  $\delta_1$  and  $\delta_2$  that were neglected in the analytical approach from section §3.1. Thus, the numerical solution can be used to validate the accuracy of the travelling wave solution. In order to have a consistent comparison with the travelling wave solution, the approximation  $u \rightarrow 1$  as  $x \rightarrow 0$  is used in the boundary condition (12a.i).

### 3.3 Results and discussion

The left panel from Fig. 1 shows the variation of the concentration of contaminant and carrier gas through the column, along with the adsorbed fraction and the velocity profile of the gas. As imposed by the boundary conditions the concentration of contaminant is close to one for large negative  $\eta$  and decreases to zero for large positive  $\eta$ . Similarly, the adsorbed fraction tends to its constant equilibrium value near the inlet,  $\hat{q} \approx 0.88$ , and to zero near the wave front where the adsorbent material is still clean of contaminant (i.e.  $\hat{q} = 0$ ). In the region of the column where the adsorbent is full of contaminant the gas velocity is highest and it decreases towards the clean region of the column, indicating that adsorption slows down the gas transport. Finally, the right panel from Fig. 1 shows the results at the outlet, comparing the numerical and travelling wave solutions. The key quantities  $\hat{c}_1$ ,  $\hat{q}$  show very good agreement, except for small times where the numerical solution is expected to be more accurate due to the inclusion of the terms with  $\delta_1$  and  $\delta_2$  which were neglected in the derivation of the travelling wave solution.

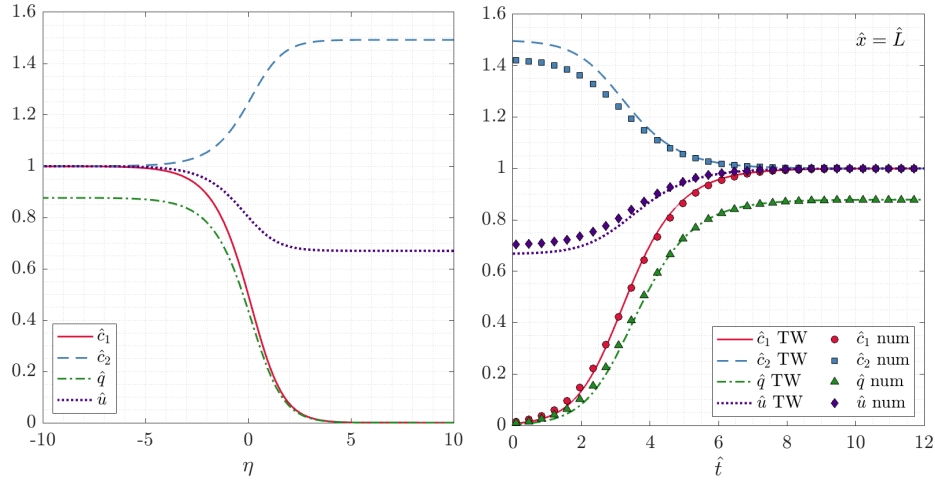


**Fig. 1.** On the left, profiles of the concentrations, adsorbed amount and velocity according to the traveling wave solutions for  $\phi_1 = 0.33$  and  $\delta_6 = 0.14$ , which is consistent with the experimental work used in §4. On the right, comparison of breakthrough curves computed numerically and via Eq. (21), using the parameter values found in Table 2 and the non-dimensional parameters provided in §4. The dimensionless half-time is  $\hat{t}_{1/2} = 3.32$ .

In Fig. 2 we show the contaminant concentration and velocity profiles for a range of volume fractions  $\phi_1$ . For 1% of contaminant, the profiles agree with fixed-velocity solution from [2]. Actually, the previous model can be obtained analytically from the present model by taking the limit  $\phi_1 \rightarrow 0$  in Eq. (19), which

yields  $\hat{c}_1 = 1 / (1 + e^{\eta/\hat{v}})$ , leading to the fixed-velocity dimensional breakthrough model of [2],

$$c_1(L, t) = \frac{c_{10}}{1 + e^{k_{ad}c_{10}(t_{1/2}-t)}}. \quad (22)$$

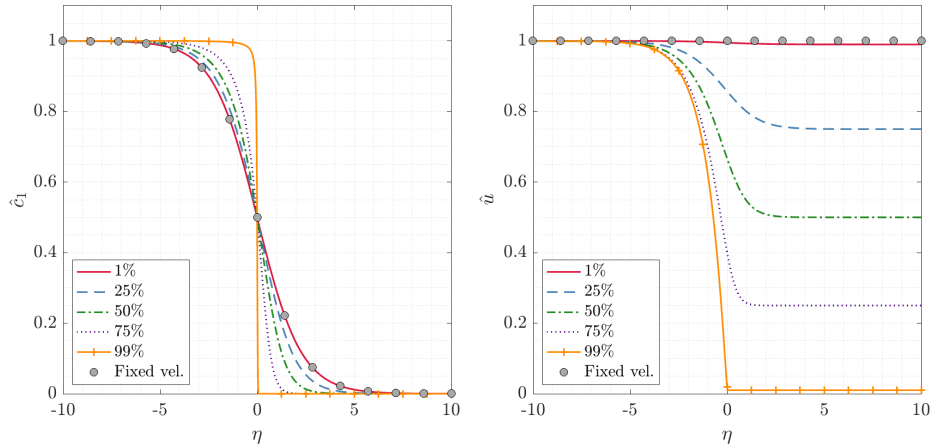


**Fig. 2.** Evolution of the contaminant concentration and gas velocity in terms of the traveling wave co-ordinate for different volume fractions  $\phi_1$  and  $\delta_6 = 0.14$ . The circles represent the solution of the fixed-velocity model described in [2].

For small values of  $\phi_1$ , from Eq. (14.ii) we find

$$\hat{u} = (1 - \phi_1) (1 + \phi_1 \hat{c}_1 + \mathcal{O}(\phi_1^2)) = 1 - \phi_1(1 - \hat{c}_1) + \mathcal{O}(\phi_1^2), \quad (23)$$

and thus the constant velocity is recovered at leading order. Conversely, for large values of  $\phi_1$  we find that both the velocity and contaminant concentration tend to constant values at either side of the wavefront, indicating a small boundary layer around the origin  $\eta = 0$  for  $\phi_1 \rightarrow 0$ . We can observe how the maximum velocity variation  $\Delta \hat{u}$  is directly related to the volume fraction occupied by the contaminant:

$$\Delta \hat{u} = \hat{u}(-\infty) - \hat{u}(\infty) = \phi_1, \quad (24)$$

which provides a justification for using the variable-velocity model when the volume fraction is significant.

## 4 Application to CO<sub>2</sub> capture

We now validate the variable-velocity model against experimental data. For this we use the experimental data of Monazam *et al.* [7], who capture CO<sub>2</sub> using polyethylenimine (PEI) modified silica from a gas mixture formed by the contaminant and N<sub>2</sub> at 90 °C. The relevant operating conditions are summarized in Table 1.

**Table 1.** Operating conditions and fluid parameter values from [7]. Isotherm parameters calculated by interpolating the values at 80°C and 100°C provided in [8]. Leading order inlet concentrations are computed using Eq. (1).

Property	Symbol	Units	Value
Column length	$L$	m	0.254
Effective density	$\rho_q$	kg/m <sup>3</sup>	2100
Dispersion coef.	$D$	m <sup>2</sup> /s	$4.8 \times 10^{-5}$
Inlet fluid vel.	$u_0$	m/s	0.0944
Ambient pressure	$p_a$	Pa (Atm)	101325 (1)
Temperature	$T$	K	363.15
Gas viscosity	$\mu$	Pa·s	$2.07 \times 10^{-5}$
Permeability	$\kappa$	m <sup>2</sup>	$2.76 \times 10^{-11}$
CO <sub>2</sub> /N <sub>2</sub> inlet conc.	$c_{10}/c_{20}$	mol/m <sup>3</sup>	11.18/22.38
CO <sub>2</sub> /N <sub>2</sub> vol fraction	$\phi_1/\phi_2$	-	0.333/0.667
Final adsorbed fraction	$q_e$	mol/kg	2.21
Max. adsorbed fraction	$q_m$	mol/kg	2.52
Equilibrium constant	$K$	m <sup>3</sup> /mol	0.65

In Fig. 3 we have fitted the value of  $k_{ad}$  for both the new and previous models of Eqs. (21) and (22), with the optimization results shown in Table 2. By comparing the error values, we can observe that the present model is more accurate than the fixed-velocity model. The accuracy is especially high for small times, indicating that the reduction in velocity during the process (shown in Fig. 2b) is significant. If the ratio of concentrations  $\phi_1/\phi_2$  were to increase we anticipate that the fitting of equation (22) would become less accurate while the present model would remain accurate. The non-dimensional parameters are  $\delta_1 = 2.11 \times 10^{-3}$ ,  $\delta_2 = 2.05 \times 10^{-2}$ ,  $\delta_3 = 1.48 \times 10^{-2}$ ,  $\delta_4 = 0.667$ ,  $\delta_5 = 0.499$ , and  $\delta_6 = 0.138$ . Their orders of magnitude clearly justify the traveling wave approach.

**Table 2.** Comparison between the fitting to Monazam *et al.* [7] breakthrough data of the variable and constant velocity models for 90°C.

Parameter	Value ( <i>u</i> var.)	Value ( <i>u</i> cons.)
$k_{ad}$ (m <sup>3</sup> mol <sup>-1</sup> s <sup>-1</sup> )	$5.352 \times 10^{-4}$	$6.753 \times 10^{-4}$
SSE	0.0245	0.0611
R-squared	0.9976	0.9941

## 5 Conclusion

We have presented an extension to the basic Langmuir adsorption model that accounts for the removal of large amounts of contaminant, such that the fluid velocity is variable. The solutions obtained using the traveling wave approach

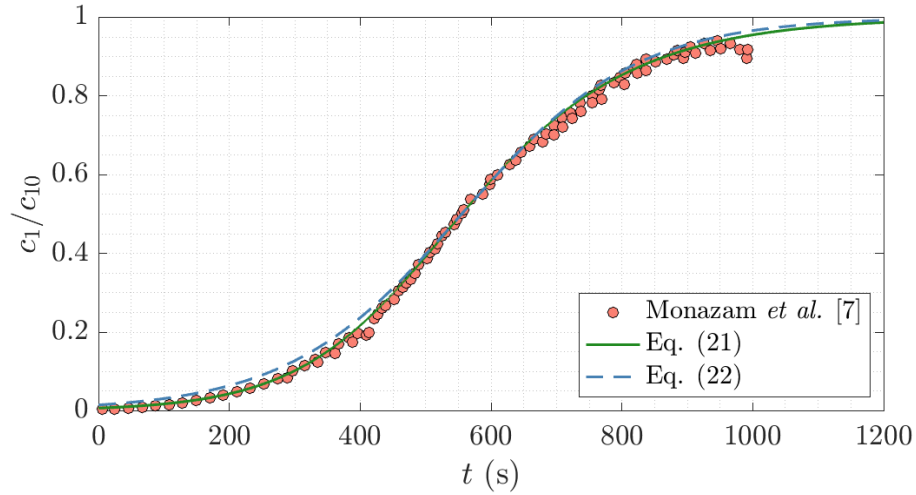


**Fig. 3.** Fitting of the model to the breakthrough data reported by Monazam *et al.* [7], using fixed and variable velocity models, at 90°C, 30 standard L/min and 33.3% of CO<sub>2</sub> at the inlet flow.

are consistent with the fixed-velocity model in [2]. The model is restricted to small pressure drops, which yield approximately constant inlet concentrations for fixed volume fractions. In practise, this does not represent a limitation, since the relevant experiments show very slow velocities and hence small pressure drops.

The experimental section provides evidence of the good agreement between the new model and the breakthrough data from a column adsorption process for the capture of CO<sub>2</sub>. In particular, the agreement is better than for the previous fixed-velocity approach. The model presented is consistent with the results obtained by fitting the isotherm. The results show how the constant velocity model loses accuracy when trying to fit the breakthrough curve obtained with a high percentage of CO<sub>2</sub> in the inlet flow is low.

Further work will include validation with larger sets of experimental data with different volume fractions. The present model only accounts for physical adsorption, hence it will be generalized to account for chemical adsorption as well. This may be done using the Sips kinetic model, which has been recently used under the assumption of constant flow [4]. For developing industrial-scale technologies, intra-particle diffusion may also be a relevant factor to introduce in the future.

## Acknowledgements

This publication is part of the research projects PID2020-115023RB-I00 and TED2021-131455A-I00 (funding T. Myers and F. Font) financed by MCIN/AEI/

10.13039/501100011033/, by “ERDF A way of making Europe” and by “European Union NextGenerationEU/PRTR”. A. Valverde acknowledges support from the Margarita Salas UPC postdoctoral grants funded by the Spanish Ministry of Universities with European Union funds - NextGenerationEU. T. Myers acknowledges the CERCA Programme of the Generalitat de Catalunya. The work was also supported by the Spanish State Research Agency, through the Severo Ochoa and Maria de Maeztu Program for Centres and Units of Excellence in R&D (CEX2020-001084-M). F. Font is a Serra-Hunter fellow from the Serra-Hunter Programme of the Generalitat de Catalunya.

## References

1. Valverde, A., Cabrera-Codony, A., Calvo-Schwarzwalder, M., Myers, T. G.: Investigating the impact of adsorbent particle size on column adsorption kinetics through a mathematical model. *International Journal of Heat and Mass Transfer* **218**, 124724 (2024).
2. Myers, T. G., Cabrera-Codony, A., Valverde, A.: On the development of a consistent mathematical model for adsorption in a packed column (and why standard models fail). *International Journal of Heat and Mass Transfer* **202**, 123660 (2023).
3. Myers, T. G., Font, F., Hennessy, M. G.: Mathematical modelling of carbon capture in a packed column by adsorption. *Applied Energy* **278**, 115565 (2020).
4. Aguares, M., Barrabés, E., Myers, T. G., Valverde, A.: Mathematical analysis of a Sips-based model for column adsorption. *Physica D: Nonlinear Phenomena* **448**, 133690 (2023).
5. Myers, T. G., Font, F.: Mass transfer from a fluid flowing through a porous media. *International Journal of Heat and Mass Transfer* **163**, 120374 (2020).
6. Langmuir, I.: The adsorption of gases on plane surfaces of glass, mica and platinum. *Journal of the American Chemical Society* **40**(9), 1361–1403 (1918).
7. Monazam, E. R., Spenik, J., Shadle, L. J.: Fluid bed adsorption of carbon dioxide on immobilized polyethylenimine (PEI): Kinetic analysis and breakthrough behavior. *Chemical Engineering Journal* **223**, 795–805 (2013).
8. Monazam, E. R., Shadle, L. J., Miller, D. C., Pennline, H. W., Fauth, D. J., Hoffman, J. S., Gray, M. L.: Equilibrium and kinetics analysis of carbon dioxide capture using immobilized amine on a mesoporous silica. *AIChE Journal* **59**(3), 923–935 (2013).